

Dielectric Properties of Aluminium and Silver Doped Zinc Oxide Nano Powder Prepared by Solution Combustion Synthesis

A. Sangeetha^{1*}, B. M. Nagabhushan², Chanappa³, Subramani³ and Ravikiran³

¹Department of Physics, Government First Grade College, Hoskote, Bengaluru Rural - 562114, Karnataka, India; amblisangeetha@gmail.com

²Department of Chemistry, M. S. Ramaiah Institute of Technology, Bengaluru - 560054, Karnataka, India

³Government First Grade College, Yelahanka, Bengaluru - 560064, Karnataka, India; bichalvchannappa@gmail.com

Abstract

Aluminium and Silver doped Zinc Oxide nano powder were synthesized by Solution Combustion method using Sucrose ($C_{12}H_{22}O_{11}$) as fuel at 600° C. X-Ray diffraction pattern analysis confirms synthesized nano powders crystallized in single phase wurtzite structure matched with JCPDS-36-1451. Addition of dopant controls the crystallite size of the synthesized nano powder. The study of dielectric permittivity, dielectric loss, AC conductivity and impedance were investigated in the frequency range of 100Hz to 5MHz at room temperature. It is evident from the analysis that dielectric properties of the samples depends on the nature of the dopant.

Keywords: Dielectric Constant, Dielectric Loss, Zinc Oxide

1.0 Introduction

Zinc oxide nano powder have been studied widely due to its distinctive physical and chemical properties apt for various applications. It is apparent that availability of wide band gap around 3.37 eV¹ is an advantage of the material which facilitates to create new structural properties by tuning its band gap by means of doping². ZnO is well known as II-VI n-type semiconductor generally crystallizes in three different phases such as zinc blende, rock salt and wurtzite³. Hexagonal wurtzite structure is more stable at room temperature compared to other two phases⁴. ZnO finds significant applications in opto-electronic and electronic devices such as LEDs, solar cells, varistors, laser diodes etc⁵⁻⁸. Its piezo and pyroelectric properties matches for sensor and photocatalyst applications⁹. Hardness and

rigidity of ZnO makes it one of the important materials in ceramic industry. Furthermore, its attractive properties like low toxicity and biodegradability makes it suitable for biological and medicinal applications¹⁰.

Selection of synthesis method of ZnO nano powder is vital to design morphology of the particles, which is a key parameter that decides not only the quality and quantity of the product but also the structural property. ZnO powders can be synthesized from traditional solid state reaction route that takes place at elevated temperatures^{1,11-12}. Coprecipitation is a wet chemical, low temperature process of synthesis to obtain high quality nano powders. It is a reduction reaction in which reduction of salt solution is followed by precipitation of ZnO from the precursor¹³⁻¹⁵. Repetitive washing of the precipitate to removes impurities from the precipitate. PH

*Author for correspondence

of the solution, drying duration and temperature controls the nature of the final product. Sol-gel is a popular synthesis method to attain nano particles of desired dimension and form owed to its moderate synthesis conditions¹⁶⁻¹⁷. Many other fabrication techniques such as Solvothermal, hydrothermal¹⁸⁻¹⁹, microwave synthesis²⁰, mechanochemical²¹ etc., has been established in order to engineer the nature of nano particles which predominates the properties.

Dielectric properties such as dielectric constant(k), dielectric loss ($\tan\delta$) and impedance determines its suitability in the field of electronics. Specifically, value of ' k ' is an index of charge storage capacity of the material. Dielectric materials can be classified as low- k materials and high- k materials. High- k materials are used in fabrication of memory cell in memory chips, capacitors for storage of charges, MOS transistors²² and so forth. On the other hand, low dielectric materials find applications in EMI shielding²³, electrical insulation, high speed IC packing and satellite communications. Research trends in the field of nano materials show that metal oxides have gained substantial importance due to their stability and low toxicity are used in majority of the applications²⁴. ZnO is a metal oxide which is widely studied because of its availability, affordability, stability and attractive structure to meet wide range of applications²⁵. Furthermore, availability of direct band gap and electric polarizability, ZnO founds to be a very good dielectric material. Enhancement of intrinsic dielectric property of ZnO can be made by addition of dopants and by controlling the shape and size of the nano particles. Addition of transition metals in the form of impurities to ZnO can modify its electrical and optical properties due to introduction of lattice defects and local distortion²⁶. Manpreet Kaur et.al. has reported the studies on the effect of Cu and N co-doping on dielectric properties of ZnO nano particles synthesized by coprecipitation method. According to the report, structural changes has been noticed with the formation of secondary phases at higher dopant concentrations. Red shift in the band gap has been noticed due addition of dopants and dielectric properties of Cu-N doped ZnO nano particles found to be suitable for photovoltaic applications²⁷. Sajid Ali Ansari *et al.* has synthesized Co doped ZnO nano particles by solution combustion method using citric acid as a fuel. Authors has studied structural, optical and electrical properties of

the nano particles. Synthesized nanoparticles crystallized in hexagonal wurtzite structure irrespective of the concentration of the dopants and band gap increased with increase in the dopant concentration. Dielectric behaviour of the samples with respect to dopants has been analysed based on Maxwell–Wagner model²⁸. Amir Zia *et al.* presented a work on the dielectric properties of cobalt doped ZnO nano structures synthesized by coprecipitation method. Results showed considerable variation in dielectric properties and finds that material is suitable for high frequency application²⁹. MD. Parvez Ahmad *et al.* reported synthesis of carbon-doped ZnO nano particles by solid-state reaction method and studied the effect of doping on the structural and dielectric properties. Authors claim that the magnitude of dielectric constant has been magnified as a result of increase in the point defects with enhancement in ac conductivity value by 10^3 times compared to the undoped samples. Variation of ac conductivity has been explained using Jonscher's power-law³⁰. Manpreet Kaur *et al.* has prepared Indium-Nitrogen codoped ZnO nano powder via coprecipitation method showing unusual deviation in the band gap pertaining to concentration of the dopant. This unusual variation has been attributed to lattice strain and the defects. Frequency dependent dielectric behaviour of the samples has been elucidated by Maxwell-Wagner model. Dielectric studies show that In-N doped ZnO particles may be used in photovoltaic and dye-sensitized solar cells applications³¹. Zulfqar *et al.* explored dielectric properties of cobalt and manganese co doped ZnO particles fabricated using chemical precipitation technique. It has been found that, increase in the calcination temperature reduced the grain boundaries which increased the ac conductivity³². M. Mehedi Hassan *et al.* successfully synthesized Fe doped ZnO particles by citrate gel method. Frequency dependent dielectric variation of the material has been explained using Maxwell–Wagner model and Koops phenomenological theory³³. Yosef Badali *et al.* reported a study on dielectric properties of Au/ZnO/n-Si structures prepared by RF sputtering method³⁴.

In the present work, dielectric properties such as dielectric constant (Real and Imaginary Part), Impedance (Real and Imaginary Part), dielectric loss ($\tan\delta$) and ac conductivity of Al and Ag doped ZnO nano particles synthesized by solution combustion method were studied. Variation of the above mentioned parameters

as a function of frequency of Al-doped, Ag-doped and Al-Ag co-doped ZnO nano powders has been analysed.

2.0 Experimental

2.1 Materials Used

Analytic reagent grade salts with 99% purity were used for the synthesis. Zinc Nitrate ($\text{Zn}(\text{NO}_3)_2 \cdot 6\text{H}_2\text{O}$), Aluminium Nitrate ($\text{Al}(\text{NO}_3)_3 \cdot 9\text{H}_2\text{O}$) and Silver nitrate (AgNO_3) were used for the synthesis of ZnO nano powder using sucrose ($\text{C}_{12}\text{H}_{22}\text{O}_{11}$) as a fuel.

2.2 Synthesis Method

Nanocrystalline ZnO powders were prepared via solution combustion technique which is a wet chemical route. Stoichiometric amount of precursors in the form of nitrates along with the fuel were initially dissolved in 10 ml of double distilled water and then continuously stirred on a magnetic stirrer for about 15 minutes to get a homogeneous solution. After that the mixture has been placed in a pre-heated furnace at 600°C . As the mixture starts boiling, water content in it gets completely evaporated forming a gel and gets ignited with a flame which is a self-propagating process. Obtained Fluffy voluminous powder has been grided using agate and mortar to get final product ready for further analysis.

2.3 Preparation of Pellets

Pellets of the synthesized ZnO nano powder were prepared for dielectric measurements. About 0.15 g of ZrTiO_4 powder has been transferred to pelletizer and pressure of about 5 tons has been applied for about 5 minutes to form a circular pellets in the form of disc. Pellets were coated with silver paste for the dielectric measurements.

2.4 Instruments Used

Bruker D8 Advance diffraction system has been utilised for structural analysis and to determine crystallite size of the samples. Fourier Transform Infra-Red (FTIR) spectroscopic measurements has been carried out using Perkin Elmer instrument. Band gap determination has been done by recording absorbance spectra of the

samples using Lambda 385 Perkin Elmer UV-Visible spectrophotometer. Nano powder has been pelletized by pressing it using hydraulic press (Shimadzu, Japan). AC electrical conductivity measurements were made using WAYNE KERR 6500B apparatus.

3.0 Results and Discussion

3.1 X-Ray Diffraction Analysis

Figures 1a, 1b, 1c, and 1d shows XRD pattern ZnO, Al-ZnO, Ag-ZnO and Al/Ag-ZnO. XRD spectra of the pure ZnO nano particles shown in Figure 1a has been crystallised in hexagonal wurtzite structure with all the peaks matched with JCPD no. 36- 1451. Crystallite size calculated using Debye Scherrer's formula are found to be around 32.63nm by taking the prominent peak of 2θ at 36.20° .

XRD pattern of Al-ZnO nano composite with 5 mol% of Al are shown in Figure 1b. All the peaks are in good agreement with those of the hexagonal wurtzite ZnO structure (JCPD no. 36- 1451). No peaks related to Al or Al_2O_3 has been recognized which clearly specifies the incorporation of Al^{3+} ions into the ZnO lattice by essentially replacing Zn^{2+} . Intensity of the peaks has been considerably reduced associated with peak broadening, indicating the stress introduced in the lattice which might be due to local distortion in the lattice structure due to addition of dopants. Substitution of smaller Al^{3+} ions in the place of larger Zn^{2+} ions reduces the process of crystallization and hence crystallite size reduced significantly compared to undoped ZnO and are found to be around 1.453nm. The existence of more defects greatly decreases the grain size.

Figure 1c illustrates XRD pattern of Ag-ZnO nano composite with 5 mol% of Ag. Majority of the peaks are identified and matched with JCPDS No. 36-1451 which are concerned to crystalline hexagonal wurtzite phase of ZnO. However, additional diffraction peaks are concerned to Face-Centred Cubic (FCC) phase of Ag (JCPDS Card No. 04-0783). This indicates that Ag ions are not being substituted in the host ZnO matrix and are likely to be embedded on the ZnO surface forming Ag:ZnO like composite material. It may be due to the larger mismatch in the ionic radii of Ag^{1+} being 1.26 \AA and that of Zn^{2+} is 0.74 \AA . Another reason could be

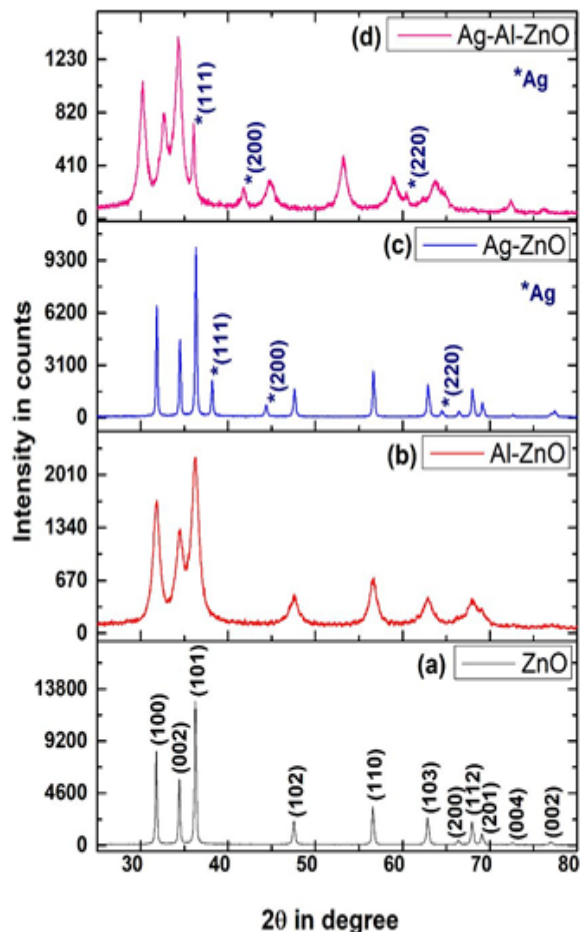


Figure 1. X-Ray diffraction pattern.

insolubility of Ag in ZnO. Accordingly, secondary phase peaks of Ag appear along with the peaks due to ZnO³⁵. Since Ag appear as a subsidiary phase along with ZnO the process of crystallization will be not affected and hence crystallites are 34.51nm in size which bigger as compared to Al-doped samples.

Figure 1d illustrates XRD of Al-Ag-ZnO nano composites with 5 mol% of Al and 5 mol% of Ag. According to XRD pattern, only peaks due to ZnO and Ag are noticed with decreased intensity of the peaks and peak broadening. This indicates that Al ions has successfully occupied Zn²⁺ site where as Ag¹⁺ ions do not occupy Zn²⁺ sites and occur as subsidiary phase. Addition of dopants into ZnO lattice has caused noticeable shifting of peak positions towards lower side signifying the presence of tensile stress that has been occurred due to lattice distortion. Such kind of peak shifting and lattice distortion with increase in the lattice constants has been

reported in the literature^{36,37}. Crystallization process has been decreased due to the presence of Al³⁺ ions and are found to be around 1.63nm.

3.2 IR Spectroscopy

Figure 2 shows the variation in optical transmittance of pure ZnO, Al-ZnO, Ag-ZnO and Al-Ag-ZnO samples. It is evident all the samples exhibit highly transparent behavior for wavenumber ranging from 500 to 4000 m⁻¹. Addition of dopants has not changed the transmittance property of ZnO drastically. Whereas small increase in the transmittance has been noticed due to addition of Al and Al-Ag, which may be attributed to reduction in the scattering due to reduced grain size. Hence high transparency of both undoped and doped ZnO can be made useful in the applications related to opto-electronics.

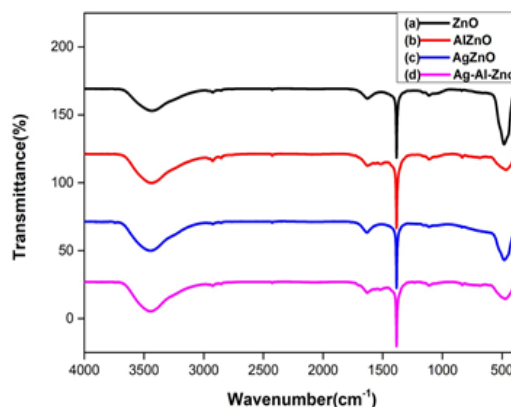


Figure 2. Fourier Transform Infrared spectra.

3.3 Uv-Visible Spectroscopy

Figure 3 illustrates optical absorption spectra of ZnO, Al-ZnO, Ag-ZnO and Al-Ag-ZnO samples. UV-Vis absorption spectra has been recorded in the wavelength range between 300nm to 800nm. Deviation in the value of band gap because of addition of dopants has been determined by Tauc method. Measured values of band gaps are found to be --- eV, --- eV, --- eV and --- eV. Accordingly, doping of P-type of impurities in particular decreases the band gap. As a consequence of doping, new impurity levels are introduced between conduction and valence bands that arise due to oxygen vacancies. These impurity states are more delocalized which overlap with

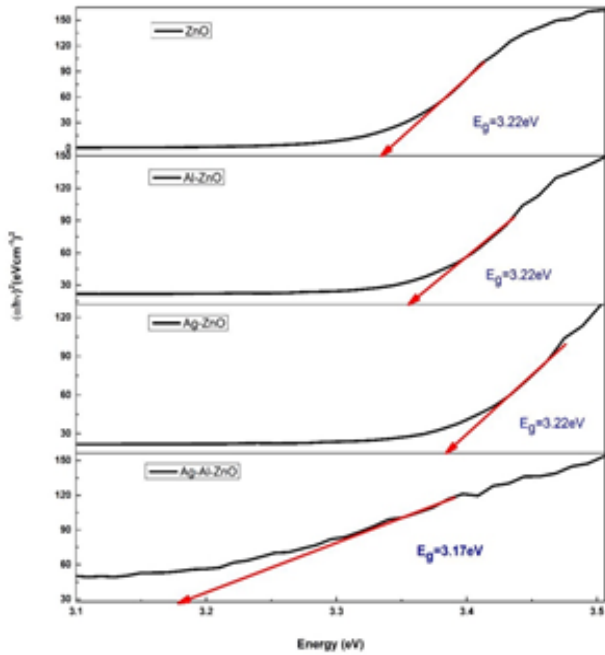


Figure 3. UV-Visible spectra. the valance band edge of ZnO leading to narrowing of band gap³⁸.

3.4 Dielectric Properties

For a given material, dielectric properties are of two types (i) Static dielectric property and (ii) Dynamic dielectric property. Static dielectric properties are simply related to behaviour of the dielectric properties of the material at low frequency or constant electric fields, whereas dynamic dielectric properties are measurements at very high frequencies with varying electric fields. Dielectric properties of the prepared samples has been explored by recording variation of dielectric constants ϵ' , ϵ'' electrical conductivity σ_{ac} , dielectric loss $\tan\delta$ and impedances Z' , and Z'' with respect to frequency between 100 Hz to 5 MHz.

3.4.1 Dielectric Constant

ZnO nano powder is a polar compound which is electrically neutral and exhibits permanent dipole moment. Dipole moment which arises due to displacement of centre of symmetry of electron cloud and nucleus is frequency sensitive because of which dielectric properties changes substantially. There are two parts of dielectric constant real part ϵ' and imaginary part ϵ'' . Real part of dielectric

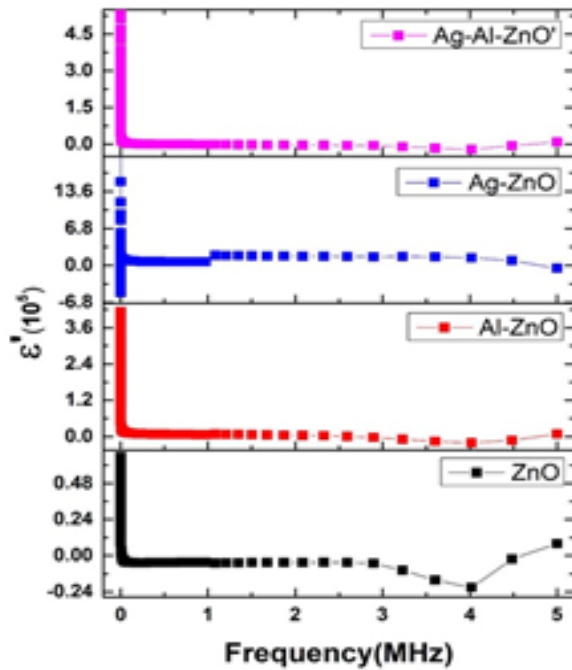


Figure 4a. Variation of ϵ' as a function of frequency.

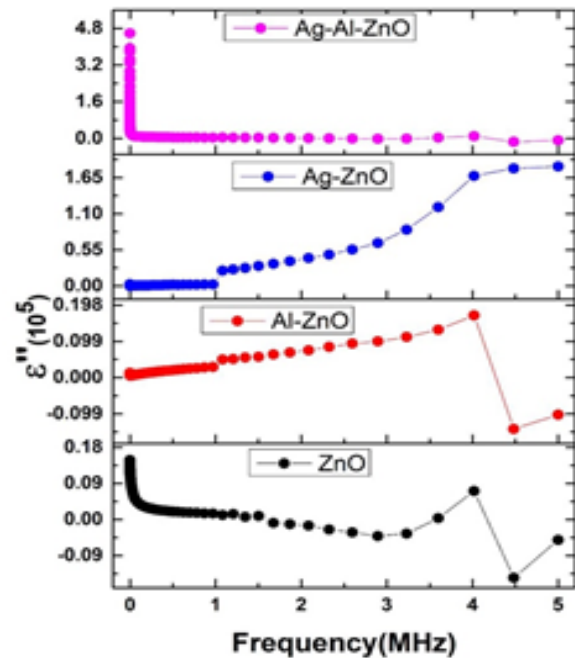


Figure 4b. Variation of ϵ'' as a function of frequency.

constant is concerned to stored energy and imaginary part of the dielectric constant describes dissipated energy in the material. Figure 4a shows variation of real

part of dielectric constant ϵ' as a function of frequency. Analysis of variation of dielectric constant with respect to frequency has been made on the basis of Maxwell–Wagner model³⁹. According to this model, dielectric medium is considered to be made up of an aggregate of large number of conducting grains with a well-defined grain boundaries basically resistive in nature. Thus with the applied external field essentially at lower frequencies, charges move freely within the grains but gets collected at the grain boundaries leading to high polarization with high dielectric constant. Structural inhomogeneity traps the electrons from hopping resulting to interfacial or space charge polarization may be considered as one more reason for the occurrence of high permittivity at low frequency region. At higher frequencies, dipoles fail to orient in the field direction at the rate of frequency variation and accumulation of the dipoles at the grain boundaries does not happen which results in lowering the value of dielectric constant^{38,40}. Addition of Al^{3+} and Ag^{1+} dopants into ZnO lattice introduces oxygen defects and creates unbalanced neutrality which increases the value of dielectric constant. Thus the dielectric constant value has been found to increase with the addition of dopants. In case of imaginary part of dielectric constant, same nature has been noticed as shown in Figure 4b. Occurrence of peaks at low and high frequency in Ag doped samples is because of synchronising of migration or hopping frequency of the charge carriers with the frequency of the applied electric field.

3.4.2 Dielectric Loss ($\text{Tan}\delta$)

Figure 5 shows the variation of $\text{tan}\delta$ with respect to frequency of pure and doped samples. Loss tangent or loss factor ($\text{tan}\delta$) gives the energy dissipation of a dielectric material. The dielectric loss of all samples decreases with increase in the frequency which is in par with the results of AC conductivity which increased with increase in the frequency. Moreover, imaginary part of the dielectric constant is directly proportional to dielectric loss and hence the imaginary dielectric constant and dielectric loss will show same behavioural pattern⁴¹. Losses are found to decrease with increasing frequency for undoped as well as doped samples. This may be due to space charge polarization of the dielectric system. Doping of Al^{3+} and co doping of Al^{3+} , Ag^{1+} decreases the value of the loss

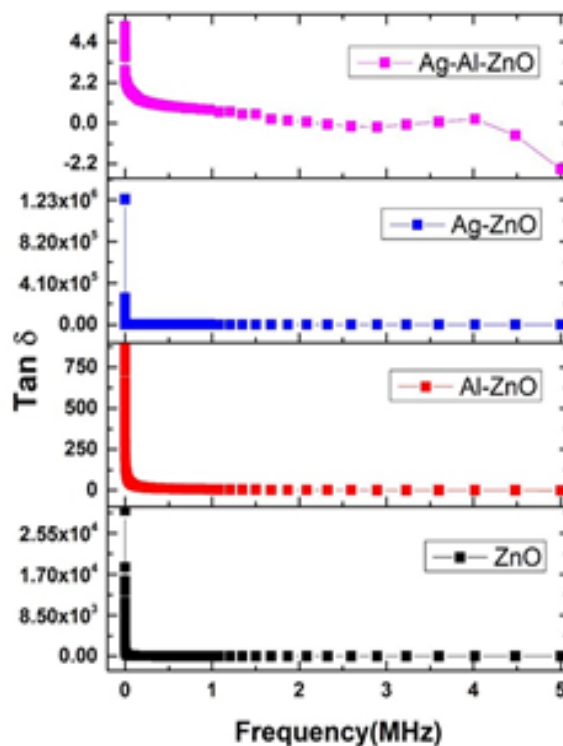


Figure 5. Variation of $\text{tan}\delta$ as a function of frequency.

whereas doping of Ag^{1+} alone increases the loss factor, the explanation for which has been discussed in AC conductivity.

3.4.3 AC Conductivity

Figure 6 shows the variation of σ_{ac} of all the samples with respect to the frequency in the 100 Hz to 5 MHz. AC conductivity shows slightly increase in the value with increase in the frequency for all the samples. According to the graph, AC conductivity for un doped sample appears to be greater than the Al^{3+} doped sample. For Ag^{1+} doped sample σ_{ac} has been hiked and for Al^{3+} and Ag^{1+} co-doped sample σ_{ac} value has decreased. AC conductivity represents ease for the mobility of the charge carriers inside the dielectric system. Due to introduction of dopant induces the defects into the system which may get accumulated near grain boundaries leading to blockage for the free flow of charge carriers. But in case of Ag^{1+} doped sample, Zn^{2+} are not replaced by Ag^{1+} which occupy interstitial sites may introduce excess charge carriers leading to higher electrical conductivity.

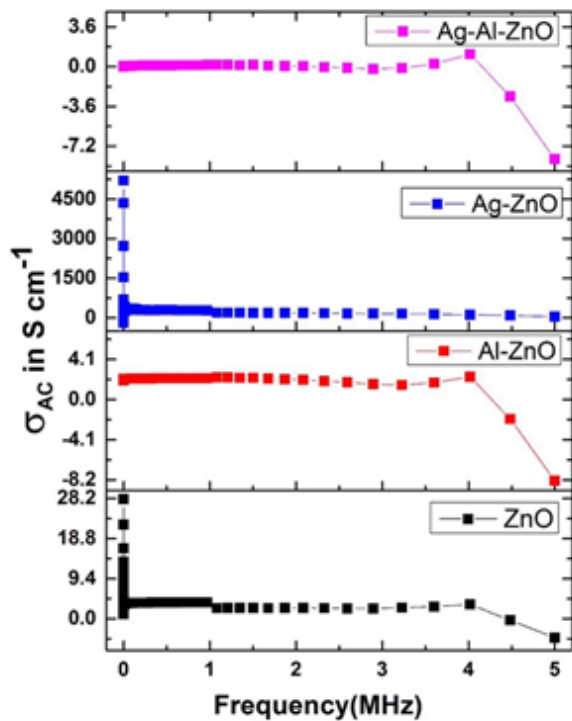


Figure 6. Variation of σ_{ac} of as a function of frequency.

3.4.4 Impedance Analysis

Figure 7a and 7b show variation of real and imaginary part of impedance with respect to frequency. Total impedance of a dielectric material is sum of resistive (real) part Z' and reactive (imaginary) part Z'' . Resistive Impedance Z' increases and reactive impedance ϵ'' increases with addition of dopants which may be attributed to the increase in the barrier height. Peaking of ZnO sample at lower frequency indicates that the frequency of orientation of the dipoles follows the frequency of the applied field. The high value of both Z' and Z'' can be assigned to resistive grain boundaries which falls suddenly with slight increase in the frequency and remains almost constant at higher frequencies over a long range²⁷.

The complex impedance plots of undoped and doped ZnO samples at room temperature is given in Figure 8. Figures illustrate the well-defined semicircles in the complex plane. This confirms the homogeneity and the single phase undoped doped samples. Furthermore, decrease in the radius of the arcs due to dopants has been observed. Cole-Cole plot of the measured impedance

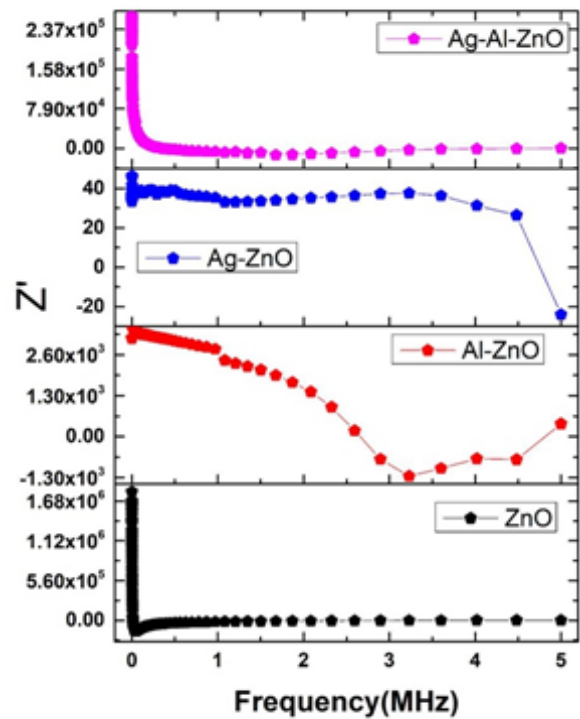


Figure 7a. Variation of Z' as a function of frequency.

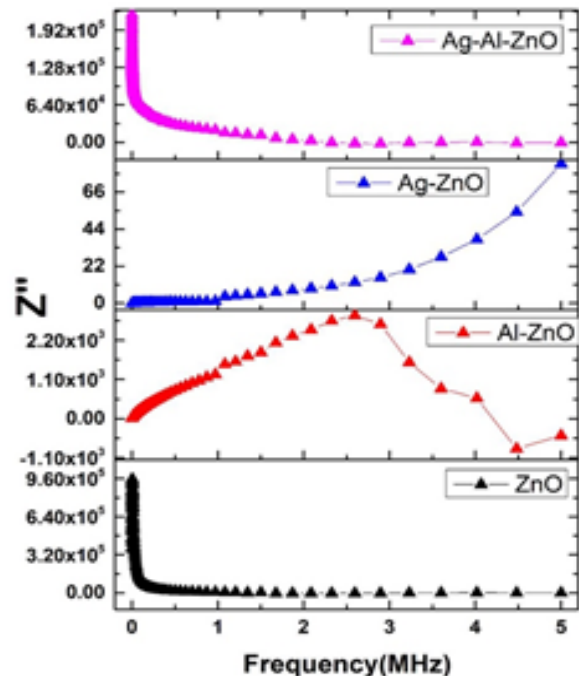


Figure 7b. Variation of Z'' as a function of frequency.

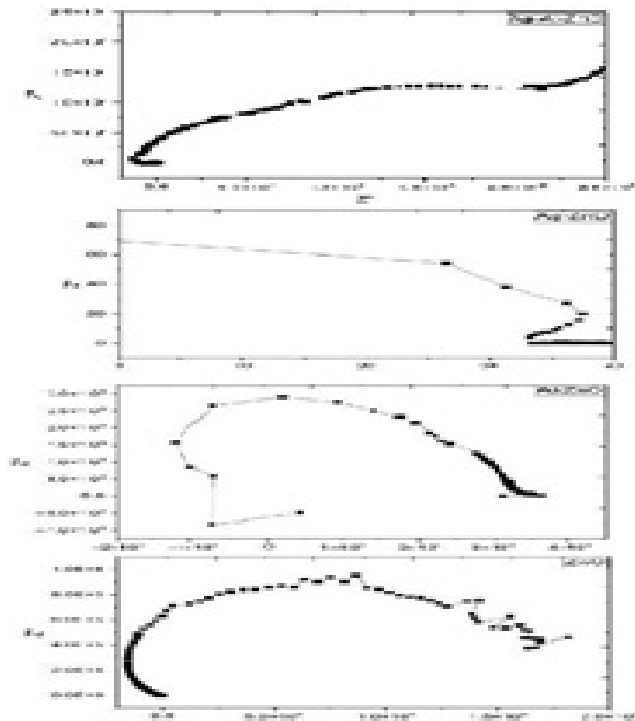


Figure 8. Variation of Z'' versus Z' .

helps to build an idea about the electrical equivalent circuit as well as the electrical phenomena inside the material. Deviation observed in the spectra is due to the inhomogeneity inside the material.

4.0 Conclusion

ZnO and Al, Ag and Al-Ag co-doped nano particles has been synthesized by energy efficient solution combustion method by using sucrose as fuel. XRD analysis clarifies ZnO exists in hexagonal wurtzite structure. Stable structure has been accomplished at low temperature without the aid of additional sintering process. Fourier transform analysis shows that pure and doped ZnO exhibits high transmittance. UV-Visible studies elaborates the structural changes that occur due to introduction of dopants by showing variation in the band gap. It is evident from the analysis of dielectric properties that all samples show frequency dependent behaviour. The dielectric properties are also found to be dopant dependent. In this study, concentration of dopant has been selected arbitrarily and therefore, there is a scope to optimise the dopant concentration to understand

dielectric nature of the material in depth. From present study, it can be concluded that synthesized samples possess very high dielectric constant with frequency independent behaviour at high frequency over a very long range. Hence the synthesized ZnO samples can be used as charge storage devices, high transmittance makes them suitable for optoelectronic devices and stable dielectric properties at high frequencies makes them promising materials for various high frequency application devices.

5.0 Acknowledgement

We acknowledge Department of Collegiate education and GFGC, Yelahanka for the encouragement to carry out this research work, MSRIT Bangalore for providing facility to carry out synthesis, Characterization and human resource for discussion and guidance. and Dr. Murugendrappa, Department of Physics, BMS Engineering College, Bangalore for extending the facility of dielectric measurements.

6.0 References

1. Kumar BR, Hymavathi B, Subba Rao T. Effect of the ceria dopant on the structural and dielectric properties of ZnO semiconductors. *J Sci Adv Mater Devices*. 2018; 3:433-439. <https://doi.org/10.1016/j.jsamd.2018.09.001>.
2. Yang J, Gao M, Yang L, *et al*. Low-temperature growth and optical properties of Ce-doped ZnO nanorods. *Appl Surf Sci*. 2008; 255:2646-2650. <https://doi.org/10.1016/j.apsusc.2008.08.001>.
3. Ul Haq B, Afaq A, Ahmed R, Naseem S. A comprehensive DFT study of zinc oxide in different phases. *Int J Mod Phys C*. 2012; 23:1250043.
4. Ashrafi A, Jagadish C. Review of zincblende ZnO: stability of metastable ZnO phases. *J Appl Phys*. 2007; 102(4).
5. Alivov YI, Kalinina EV, Cherenkov AE, *et al*. Fabrication and Characterization of n-ZnO/p-AlGaIn Heterojunction Light-Emitting Diodes on 6H-SiC Substrates. *Appl Phys Lett*. 2003; 83(23):4719-4721. <https://doi.org/10.1063/1.1632537>.
6. Kim HS, Lugo F, Pearton SJ, *et al*. Phosphorus Doped ZnO Light Emitting Diodes Fabricated via Pulsed Laser Deposition. *Appl Phys Lett*. 2008; 92(11):112108-112110. <https://doi.org/10.1063/1.2900711>.
7. Singh A, Kumar D, *et al*. *J Electrochem Soc*. 2011; 158(1):G9-G12. <http://dx.doi.org/10.1149/1.3511788>.

8. Murugadoss G. *J Mater Sci Technol.* 2012; 28(7):587–593.
9. Chaari M, Matoussi A. Electrical conduction and dielectric studies of ZnO pellets. *Phys B Condens Matter.* 2012; 407:3441–3447.
10. Özgür U, Alivov YI, Liu C, *et al.* A comprehensive review of ZnO materials and devices. *J Appl Phys.* 2005; 98. <https://doi.org/10.1063/1.1992666>.
11. Divya NK, Aparna PU, Pradyumnan PP. Dielectric Properties of Er³⁺ Doped ZnO Nanocrystals. *Adv Mater Phys Chem.* 2015; 5:287–294. <http://dx.doi.org/10.4236/ampc.2015.58028>.
12. Ahmad MP, Rao AV, Babu KS, Rao GN. Effect of carbon-doping on structural and dielectric properties of zinc oxide. *J Adv Dielectrics.* 2020; 10(4):2050017. <http://doi:10.1142/S2010135X20500174>.
13. Lanje AS, Sharma SJ, Ningthoujam RS, *et al.* Low temperature dielectric studies of zinc oxide (ZnO) nanoparticles prepared by precipitation method. *Adv Powder Technol.* 2013; 24:331–335.
14. Jayachandriah, Krishnaiah, Erbium induced raman studies and dielectric properties of Er-doped ZnO nanoparticles. *Adv Mater Lett.* 2015; 6(8):743–748. <http://doi:10.5185/amlett.2015.5801>.
15. Badreddine K, Srour A, Awad R, Abou-Aly AI. The investigation of mechanical and dielectric properties of Samarium doped ZnO nanoparticles. *Mater Res Express.* 2020; 7:025016. <https://doi.org/10.1088/2053-1591/ab7064>.
16. Vignesh K, Nair AS, Udhayakeerthana C, Kalaivani T. Synthesis and characterization of ZnO nanoparticles using sol-gel method and their antibacterial study. *IOP Conf Series: Mater Sci Eng.* 2022; 1219:012019. <https://doi:10.1088/1757-899X/1219/1/012019>.
17. Vishwakarma A, Singh SP. Synthesis of Zinc Oxide Nanoparticle by Sol-Gel Method and Study its Characterization. *Int J Res Appl Sci Eng Technol.* 2020; 8(4).
18. Mohan S, Vellakkat M, Aravind A, Reka U. Hydrothermal synthesis and characterization of Zinc Oxide nanoparticles of various shapes under different reaction conditions. *Nano Express.* 2020; 1:030028. <https://doi.org/10.1088/2632-959X/abc813>.
19. Bharti DB, Bharathi AV. Synthesis of ZnO nanoparticles using a hydrothermal method and a study its optical activity. *Luminescence.* 2016; 32(3):317–320. <https://doi:10.1002/bio.3180>. PMID: 27430489.
20. Porrawatkul P, Pimsen R, Kuyyogsuy A, *et al.* Microwave-assisted synthesis of Ag/ZnO nanoparticles using Averrhoa carambola fruit extract as the reducing agent and their application in cotton fabrics with antibacterial and UV protection properties. *RSC Adv.* 2022; 12:15008. <https://doi:10.1039/d2ra01636b>.
21. Zhou Z, Wang J, Jhun CG. ZnO Nanospheres Fabricated by Mechanochemical Method with Photocatalytic Properties. 2021; 11:572. <https://doi.org/10.3390/catal11050572>.
22. Pravin JC, Nirmal D, Prajoun P, Kumar NM, Ajayan J. Investigation of 6T SRAM memory circuit using high-k dielectrics based nano scale junctionless transistor. *Superlattices Microstruct.* 2017; 104:470–476.
23. Singh H, Kumar D, Sawant KK, Devunuri N, Banerjee S. Co-Doped ZnO-PVA Nanocomposite for EMI Shielding. *Polym-Plast Technol Eng.* <https://doi:10.1080/03602559.2015.1070869>.
24. Chavali MS, Nikolova MP. Metal oxide nanoparticles and their applications in nanotechnology. *SN Appl Sci.* 2019; 1:607. <https://doi.org/10.1007/s42452-019-0592-3>.
25. Kołodziejczak-Radzimska A, Jesionowski T. Zinc Oxide—From Synthesis to Application: A Review. *Materials.* 2014; 7:2833–2881. <https://doi:10.3390/ma7042833>.
26. Gao Q, Dai Y, Li X. Effects of mn dopant on tuning carrier concentration in Mn doped ZnO nanoparticles synthesized by co-precipitation technique. *J Mater Sci.* 2018; 295:3568–3575.
27. Kaur M, Kumar V, Singh J, Datt J, Sharma R. Effect of Cu-N co-doping on the dielectric properties of ZnO nanoparticles. *Mater Technol.* 2022. <https://doi:10.1080/10667857.2022.2055909>.
28. Ansari SA, Nisar A, Fatma B, Khan W, Naqvi AH. Investigation on structural, optical and dielectric properties of Co doped ZnO nanoparticles synthesized by gel-combustion route. *Mater Sci Eng B.* 2012; 177:428–435. <https://doi:10.1016/j.mseb.2012.01.022>.
29. Zia A, Ahmed S, Shah NA, Anis-ur-Rehman M, Khan EU, Basit M. Consequence of cobalt on structural, optical and dielectric properties in ZnO nanostructures. *Physica B.* 2015; 473:42–47. <https://doi.org/10.1016/j.physb.2015.05.024>.
30. Ahmad MP, Rao AV, Babu KS, Rao GN. Effect of carbon-doping on structural and dielectric properties of zinc oxide. *J Adv Dielectrics.* 2020; 10(4):2050017. <http://doi:10.1142/S2010135X20500174>.
31. Kaur M, Kumar V, Kaur P, *et al.* Effect on the dielectric properties due to In-N co-doping in ZnO particles. *J Mater Sci: Mater Electron.* 2021; 32:8991–9004. <https://doi.org/10.1007/s10854-021-05570-w>.

32. Zulfiqar, Zubair M, Khan A, Hua T, Ilyas N, Fashu S, Afzal AM. Oxygen vacancies induced room temperature ferromagnetism and enhanced dielectric properties in Co and Mn co-doped ZnO nanoparticles. *J Mater Sci: Mater Electron*. <https://doi.org/10.1007/s10854-021-05610-5>.
33. Hassan MM, Ahmed AS, Chaman M, Khan W. Structural and frequency dependent dielectric properties of Fe³⁺ doped ZnO nanoparticles. *Mater Res Bull*. 2012; 47:3952–3958. <http://dx.doi.org/10.1016/j.materresbull.2012.08.015>.
34. Badali Y, Altındal Ş, Uslu İ. Dielectric properties, electrical modulus and current transport mechanisms of Au/ZnO/n-Si structures. *Prog Nat Sci: Mater Int*. 2018; 28:325–331. <https://doi.org/10.1016/j.pnsc.2018.05.003>.
35. Ye XY, Zhou YM, Sun YQ, Chen J. *J Nanopart Res*. 2009; 11:1159–1166. <https://doi.org/10.1007/s11051-008-9511-z>.
36. Chakraborti D, Narayan J, Prater JT. Room temperature ferromagnetism in Zn_{1-x}Cu_xO thin films. *Appl Phys Lett*. 2007; 90:062504–062506.
37. Mass J, Bhattacharya P, Katiyar RS. Effect of high substrate temperature on Al-doped ZnO films grown by pulsed laser deposition. *Mater Sci Eng B*. 2003; 103:9–15.
38. Dey B, Narzary R, Chouhan L, Bhattacharjee S, Parida BN, Mondal A, Ravi S, Srivastava SK. Crystal structure, optical and dielectric properties of Ag:ZnO composite-like compounds. *J Mater Sci: Mater Electron*. <https://doi.org/10.1007/s10854-021-07560-4>.
39. Wagner KW. *Am Phys*. 1973; 40:817–819.
40. Zamiri R, Singh B, Belsley MS. Structural and dielectric properties of Al-doped ZnO nanostructure. *Ceram Int*. 2014; 40:6031–6036. <http://dx.doi.org/10.1016/j.ceramint.2013.11.052>.
41. Zia A, Ahmed S, Shah NA, Anis-ur-Rehman M, Khan EU, Basit M. Consequence of cobalt on structural, optical and dielectric properties in ZnO nanostructures. *Physica B*. 2015; 473:42–47. <https://doi.org/10.1016/j.physb.2015.05.024>.